Pergamon

PII: S0022-3697(98)00207-8

J. Phys. Chem Solids Vol 59, No. 10–12, pp. 2201–2204, 1998
0022-3697/98/$ - see front matter

HIGH PRESSURE STUDIES ON YNi_2B_2C AND $LuNi_2B_2C$: ADXRD, THERMOELECTRIC POWER, RESISTIVITY, AND ELECTRONIC

B. K. GODWAL[†]*, S. MEENAKSHI[†], V. VIJAYAKUMAR[†], R. S. RAO[†] and P. RAVINDRAN[‡]

[†]High Pressure Physics Division, Bhabha Atomic Research Centre, Mumbai 400085, India
[‡]Condensed Matter Theory Group, Department of Physics, Uppsala University, Uppsala, Sweden

Abstract—The electronic and structural behaviour of YNi_2B_2C and $LuNi_2B_2C$ at high pressures were investigated by electrical resistivity, thermoelectric power (TEP), and angle dispersive X-ray diffraction measurements and by electronic band structure calculations. The pressure variation of TEP shows a peak around 2 GPa in YNi_2B_2C. However, the X-ray powder diffraction does not show any structural transition up to 16.4 GPa. The equation of state of YNi_2B_2C yielded a relatively high bulk modulus of 200 GPa. The observed peak in TEP and the pressure variation of the superconducting transition temperature can be correlated with different components of the electronic density of states. The universal equation of state shows deviation from linearity around 1.5 GPa pressure and correlates well with the TEP peak. © 1998 Elsevier Science Ltd. All rights reserved

1. INTRODUCTION

The lanthanide nickel borocarbide (RNi_2B_2C where R = lanthanide) superconductors show interesting high pressure behaviour. The superconducting transition temperatures (T_c) of these materials, except $HoNi_2B_2C$, show a linear pressure dependence and the slope of T_c *versus* pressure curve (dT_c/dP) changes sign between Lu and Tm in the series [1–5]. Compression often causes changes in electron density of states at the Fermi level (E_F), phonon density of states and the structure, and thus can lead to change in T_c. These high pressure changes also affect the normal state transport properties like electrical resistance and thermoelectric power (TEP). Hence, measurements of electrical resistance and TEP under pressure for YNi_2B_2C and $LuNi_2B_2C$, and the angle dispersive X-ray diffraction (ADXRD) measurements on YNi_2B_2C were carried out to investigate the effect of pressure on these borocarbides. In addition, the first principles electronic structure calculations as a function of pressure were carried out to interpret our experimental data and the T_c behaviour mentioned above.

2. EXPERIMENTAL DETAILS

For electrical resistivity and TEP measurements, initially pellets of the samples of approximate size 0.2 × 3 × 5 mm were prepared and then pressed between tungsten carbide (WC) anvils to a load of 5 ton. The well compacted material was then trimmed to 1.5 mm long and 2.5 mm wide pieces and used for the high pressure electrical resistance and TEP measurements. An opposed Bridgeman anvil setup [6], consisting of 12 mm face diameter WC anvil pairs, two 0.15 mm thick pyrophylite gaskets and talc pressure medium, with *in-situ* Bi pressure calibration, was employed. Resistance was measured by the four probe technique. Thin maylar sheets protected the sample from direct contact with talc and also ensured good electrical contact by preventing talc from entering the sample and electrical leads. For TEP, 10 mil chromel and alumel thermocouple wires were employed [7a, 7b] and the negligible change in the thermo-emf of chromel and alumel with pressure was ignored. The thermocouple wires were held in position within the gaskets by grooves marked on it and over the sample by thin maylar sheet taped to the anvil. The ADXRD measurements employed a photostimulant fluorescent plate (imaging plate) as an area detector [8].† The sample was loaded in a Bassett type diamond anvil cell (DAC) along with ruby for pressure measurements.

3. THEORETICAL CALCULATIONS

The first principles total energy calculations by the full potential LMTO (FP-LMTO) method [9a, 9b] were carried out on YNi_2B_2C and $LuNi_2B_2C$. Barth–Hedin [10], and also, the generalized gradient approximation (GGA) [11] were employed for the exchange-correlation terms as the former gave lower (by about 6% from the

*Corresponding author. Tel: +91 22 551 3848; fax: +91 22 556 0750; e-mail: bkgodwa@magnum.barct1.ernet.in

†See Ref. [3] for details. The IP system is based on a 425E Molecular Dynamics phosphor imager model.

experimental data [12]) equilibrium volume. The basis set in FP-LMTO calculations comprised of augmented linear muffin–tin orbitals containing 4s, 4p, 5s, 5p, 4d, 4f of Y (5s, 5p, 6s, 6p, 5d, 5f of Lu), 3p, 3d, 4s, 4p of Ni, 2s, 2p and 3d of B and C. Further, two sets of energy parameters, one with energies appropriate to the semicore bands and the other for the valence bands were used to calculate the radial functions in the muffin–tin spheres. Also, two tail energies were used for every state. Approximate orthogonality between bases with the same l value was maintained by energy separation. Integration over the BZ was done using ''special point sampling'' [13a, 13b]. The results reported here used 75 **k**-points in the irreducible wedge of the BZ. The total energies at various volume fractions were fitted to a polynomial to calculate the pressure.

Also, as the atom and orbital decomposition of the electron density of states (DOS) is not well defined in FP-LMTO, these details were studied by the tight binding LMTO (TB-LMTO) method [14] with atomic sphere approximation (ASA) using Barth–Hedin exchange. These calculations employed the scalar relativistic terms and frozen core. The Y\Lu ($4d^15s^2\backslash 5d^16s^2$), Ni ($3d^94s^1$), B ($2s^22p^1$), and C ($2s^22p^2$) levels were treated as valence electron states. The measured data on lattice constant and atomic positions [12] were employed while the atomic sphere radii ratios used were Y:Ni:B:C = 1.0:0.79:0.52:0.5. Also, the combined correction terms, which account for the nonspherical shape of the atomic cells and the truncation of higher partial waves, were included. The eigenvalues were obtained with a set of 349 **k**-points for **k**-summation (tetrahedron method).

4. RESULTS AND DISCUSSION

The electrical resistance of YNi_2B_2C showed a rapid decrease up to about 2 GPa, and a smooth weak pressure dependence thereafter up to about 8 GPa (see Fig. 1 of Ref. [15]) suggesting the absence of structural phase transition. But in the TEP measurements we find a peak around 2 GPa pressure (see Fig. 1), signalling possible change in the electronic density of states at the Fermi level (E_F), and/or changes in the Fermi surface topology [16a, 16b, 16c]. Our ADXRD measurements showed that there is no structural transition and the ambient tetragonal structure (space group I4/mmm) is retained up to 16.4 GPa. It is seen from Fig. 2 that the equation of state (EOS) obtained from FP-LMTO with GGA agrees very well with the experimental data. The P–V data yielded the bulk modulus of about 200 GPa. The calculated equilibrium volume is within 2% of the experimental value. The computed EOS (Fig. 2), and the measured electrical resistivity of $LuNi_2B_2C$ under compression show identical behaviour, but no appreciable peak in TEP was observed. Further detailed comparison

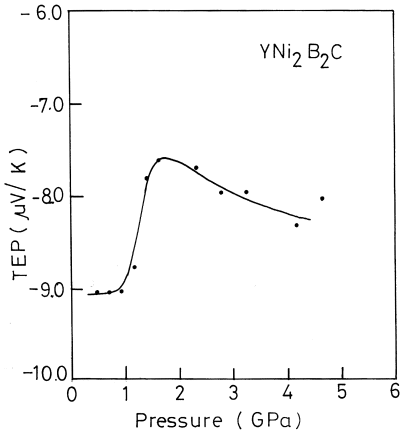

Fig. 1. Variation of the thermoelectric power of YNi_2B_2C with pressure. Measured data points are shown by filled circles and a smooth curve is drawn to indicate the variation.

of the calculated electronic structures of these two systems are being carried out to understand these details.

The analysis of (TB-LMTO) results, show that the boron component of the DOS gets reduced at E_F at high pressures. The DOS peak in the vicinity of E_F moves slowly away from it (see Fig. 3). The T_c is influenced by the boron component of DOS at E_F as these states couple strongly to the phonons involving boron displacements in the NiB_4 tetrahedra [17]. Thus, our calculations qualitatively explain the decrease of T_c with pressure in YNi_2B_2C. Note that the electron energy bands in Ref. [17] show that the boron component peak in $LuNi_2B_2C$ is just below E_F. Under pressure, this peak would move closer to E_F and the subsequent increase in DOS at E_F would increase T_c in $LuNi_2B_2C$. But T_c decreases in $TmNi_2B_2C$ and $ErNi_2B_2C$ under compression [5]. Thus by similar reasoning, the boron component of DOS peaks in them are expected to be just above E_F as in YNi_2B_2C.

The TEP data, should be dominated by the *d*-component of the DOS as in the transition metals

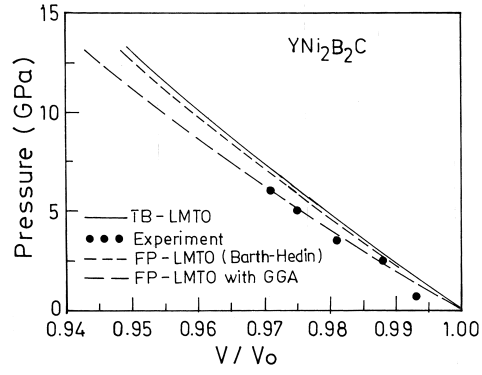

Fig. 2. Equation of state for YNi_2B_2C. The FP-LMTO calculations (with Barth–Hedin exchange-correlation terms) on $LuNi_2B_2C$ give identical curve as for YNi_2B_2C, and hence not shown separately.

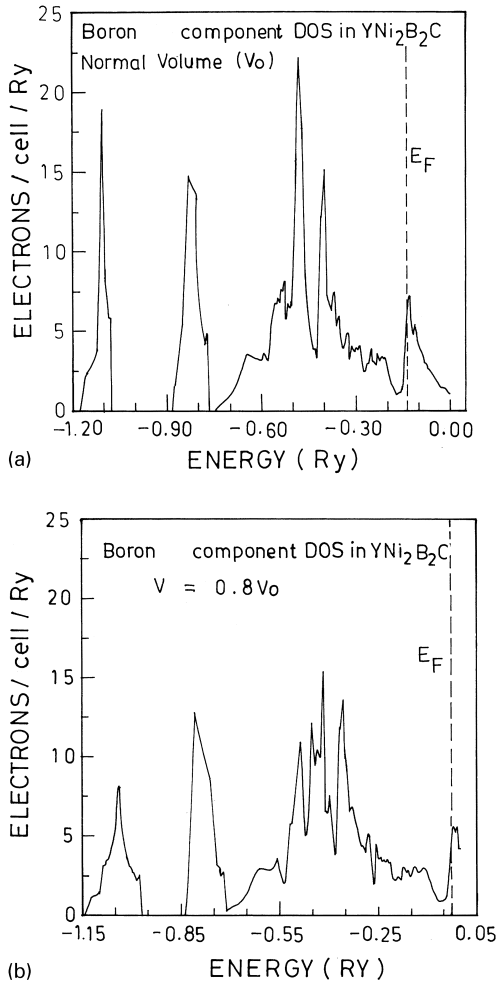

Fig. 3. Boron component density of states of YNi_2B_2C at (a) normal volume, and (b) relative volume ratio $V/V_0 = 0.8$.

[18]. Our calculations show a sharp peak in the vicinity of E_F in the Ni component of DOS (not shown). This peak slowly gets displaced to higher energies, away from E_F as pressure increases. Thus, we conjecture that the observed broad peak in TEP is due to the slow shift of the Ni *d*-based bands through E_F to higher energies (from occupied to unoccupied region). Interestingly, the universal EOS shown in Fig. 4 exhibits deviation from linearity, indicating electronic transitions, around 1.5 GPa pressure, which correlates well with the TEP peak.

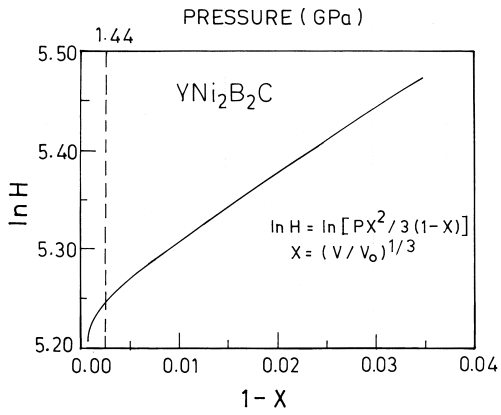

Fig. 4. Universal equation of state for YNi_2B_2C. The variables X and H are related to relative volume V/V_0 and pressure P as shown in the legend. The pressure at which the deviation from linearity occurs is marked at the top.

In summary, we have presented high pressure investigations at room temperature of the borocarbide superconductors, YNi_2B_2C and $LuNi_2B_2C$ by electrical resistivity (up to 8 GPa) and thermoelectric power (up to 5 GPa). The angle dispersive X-ray diffraction measurements (up to 16.4 GPa) were carried out on YNi_2B_2C. The electrical resistivity and ADXRD measurements show that no structural transition takes place in the measured pressure range. The pressure volume data yield a relatively high bulk modulus of 200 GPa which is corroborated by the first principles electronic structure and total energy calculations by TB-LMTO and FP-LMTO methods. The observed broad peak in the TEP measurement at about 2 GPa pressure is interpreted in terms of the shift of the Ni *d*-based bands through E_F to higher energies. Further, the fall of T_c with pressure is explained in terms of the reduction in the DOS at E_F of the boron component peak due to its slow shift from E_F.

Acknowledgements—We thank Z. Hossain, R. Nagarajan, L. C. Gupta and R. Vijayaraghavan for many useful discussions and for providing us with the borocarbide samples. One of the authors (PR) wishes to acknowledge B. Johansson, O. Eriksson and J. M. Wills for the encouragement.

REFERENCES

1. Nagarajan, R., Mazumdar, C., Hossain, Z., Dhar, S. K., Gopalakrishnan, K. V., Gupta, L. C., Godart, C., Padalia, B. D. and Vijayaraghavan, R., *Phys. Rev. Lett.*, 1994, **72**, 274.
2. Cava, R. J., Takagi, H., Zandbergen, H. W., Krajewski, J. J., Peck, W. F., Siegrist, T., Batlogg, B., Van Dover, R. B., Felder, R. J., Mizuhashi, K., Lee, J. O., Elsaki, H. and Uchida, S., *Nature*, 1994, **367**, 252.
3. Meenakshi, S., Vijayakumar, V., Godwal, B. K., Sikka, S. K., Hossain, Z., Nagarajan, R., Gupta, L. C. and Vijayaraghavan, R., *Physica B*, 1996, **223/224**, 93.
4. Ravindran, P., Shankaralingam, S. and Asokamani, R., *Phys. Rev. B*, 1995, **52**, 12921.
5. Schmidt, H. and Braun, H. F., *Physica C*, 1994, **229**, 315.
6. Vijayakumar, V., Godwal, B. K., Vohra, Y. K., Sikka, S. K. and Chidambaram, R., *J. Phys. F*, 1984, **14**, L65.

7a. Singh, A. K. and Ramani, G., *Rev. Sci. Instrum.*, 1978, **49**, 1324.

7b. Vijayakumar, V., Vaidya, S. N., Sampathkumaran, E. V. and Gupta, L. C., *High Temp.–High Press.*, 1980, **12**, 649.

8. Shimomura, O. and Takemura, K., *Rev. Sci. Instrum.*, 1992, **63**, 967.

9a. Wills, J. M. and Cooper, B. R., *Phys. Rev. B*, 1987, **36**, 3809.

9b. Price, D. L. and Cooper, B. R., *Phys. Rev. B*, 1989, **39**, 4945.

10. Von Barth, U. and Hedin, L., *J. Phys. C*, 1972, **5**, 1629.
11. Perdew, J. P., Chevary, J. A., Vosko, S. H., Jackson, K. A., Pederson, M. R. and Singh, D. J., *Phys. Rev. B*, 1992, **46**, 6671.

12. Chakoumakos, B. C. and Paranthaman, M., *Physica C*, 1994, **227**, 143.
13a. Chadi, D. J. and Cohen, M. L., *Phys. Rev. B*, 1973, **8**, 5747.
13b. Froyen, S., *Phys. Rev. B*, 1989, **39**, 3168.
14. Andersen, O. K. and Jepsen, O., *Phys. Rev. Lett.*, 1984, **53**, 2571.
15. Meenakshi, S. *et al*., in press.
16a. Lifshitz, L. M., *Sov. Phys. JETP*, 1960, **11**, 1130.
16b. Dagens, L., *J. Phys. Lett. (Paris)*, 1976, **37**, 137.
16c. Dagens, L., *J. Phys. F*, 1978, **8**, 2093.
17. Mattheiss, L. F., Siegrist, T. and Cava, R. J., *Solid-State Commun.*, 1994, **91**, 587.
18. Blatt, F. J., Schroeder, P. A., Foiles, C. L. and Greig, D., *Thermoelectric Power of Metals*. Plenum Press, New York, 1976.